THE AMERICAN SOCIETY OF MECHANICAL ENGINEERS
345 E. 47th St., New York, N.Y. 10017

95-GT-336

PREDICTION OF COMBUSTION INDUCED OSCILLATIONS USING A PRESSURE-CORRECTION METHOD

Ren Liu & James J. McGuirk

Department of Aeronautical and Automotive Engineering and Transport Studies
Loughborough University of Technology
Leicestershire, LE11 3TU
United Kingdom

ABSTRACT

The objective of the present paper is to describe the development and testing of a CFD method based on a pressure-correction formulation for the prediction of reheat-buzz-type combustion induced oscillations. A quasi-1D approach was adopted to describe the acoustic phenomena occurring in a typical premixed flame stabilised on a conical gutter. Experimentally deduced unsteady heat release data available in the published literature were used to drive the calculations. Excellent agreement was observed between measured and predicted mode shapes and phase distributions of the unsteady pressure field. Calculations also indicated that the measured buzz frequencies could be reasonably well predicted.

NOMENCLATURE

A	duct cross-sectional area
c_p	specific heat at constant pressure
f	a general flow variable
h_t	total enthalpy
L	duct length (see Figure 1)
M_{ref}	mean Mach number at reference position
p	static pressure
p_{atm}	atmospheric pressure
p_{tot}	total pressure
p'	pressure perturbation
q	heat source
R	gas constant (287 J/(kg K))
T	temperature
T_{ref}	reference temperature
T_{tot}	total temperature
t	time
u	velocity
x	spatial coordinate along duct axis
x_G	gutter lip position (see Figure 1)
x_{ref}	reference position
α	angle
Δt	time step
$\Delta_{i+1/2}$	$= (f_{i+1} - f_i)/(x_{i+1} - x_i)$
Δ^+, Δ^-	limited value of $\Delta_{i+1/2}$ etc. (see Eqs. (8), (9))
ρ	density
Subscript	
i	grid index of finite volume centre

INTRODUCTION

Computational fluid dynamics (CFD) methods have for some time now been successfully used in the calculation of steady-state incompressible combusting flows in gas-turbine engines (McGuirk, 1990). On the other hand, important combustion problems involving flow unsteadiness and compressibility effects have so far received very little attention from the viewpoint of CFD modelling and have had to be addressed primarily via experimental studies (AGARD CP No. 450, 1988). One long-standing problem in combustion systems is the occurrence of sustained pressure oscillations accompanying the combustion process, normally referred to as combustion instabilities. Sustained disturbances which find their origins in combustion instability have been observed to occur in many combustion systems, such as rockets, ramjets and gas-turbine engines. Combustion oscillations can be caused by, for example, fluctuations in the mass flow rate of fuel and/or air, changes in the rates of fuel atomization and vaporization, or vortex shedding from baffles acting as flameholders. A particularly interesting type of combustion oscillation, commonly called reheat buzz, occurs in the reheat system used in aero-engine afterburners. This is an acoustically coupled, low frequency oscillation (typically 50 - 200 Hz) caused by a resonant interaction between the combustion process and the axial propagation of

Presented at the International Gas Turbine and Aeroengine Congress and Exposition
Houston, Texas - June 5-8, 1995

acoustic waves. Rayleigh's criterion (Rayleigh, 1896) for the development of combustion driven oscillations states that acoustic waves gain energy from unsteady combustion if the fluctuations in the unsteady heat release rate are in phase with the acoustic waves. Therefore, the amplitude of oscillations can increase if the energy gained from unsteady heat release exceeds that lost to boundaries. Reheat buzz must be given appropriate consideration in the design of afterburner systems since, if left unchecked, large amplitude pressure fluctuations can occur, which may cause structural damage, or result in shortening of component lifespan due to fatigue. The development of a suitable CFD model for this kind of phenomenon would lead to an improved understanding of this important and challenging scientific problem, but also to a considerable technological advantage by helping to provide more effective design methods.

Recently, buzz oscillations in a laboratory model of an afterburner have been studied both experimentally and theoretically (Langhorne, 1988, Bloxsidge et al., 1988, and MacQuisten and Dowling, 1993, hereafter collectively referred to as LBM). This series of experiments has been selected here for particular study, since the conditions of the experiment were clearly controlled and specified, allowing convenient numerical modelling. However, these measurements are typical of a large body of literature which has examined similar phenomena in a wide range of practically relevant geometries and flow conditions (e.g. Katsuki and Whitelaw, 1986, Sivasegaram and Whitelaw, 1987, Yu et al., 1991). The experimental facility used in LBM consisted of a confined, premixed, turbulent flame stabilized in the wake of a conical bluff body. Two types of instability were observed. In the first kind, perturbations in heat release rate were convected downstream at approximately the velocity of the reactants, producing a linear phase distribution for the unsteady heat release rate. The phase of pressure perturbations was, in contrast, almost constant in the flame. In the second type of instability, the phase of the unsteady heat release rate was constant and close to that of the pressure fluctuations. In this case very intense oscillations resulted. It is not obvious what controls the appearance of the two types of instability and this question is left open in the report of these experiments (Bloxsidge et al. (1988)). Based on experimental observations, Bloxsidge et al. (1988) developed an empirical flame model describing flame response to flow perturbations. This flame model related the unsteady heat release rate at the flameholder to local velocity perturbations, the Strouhal number and the mean flow conditions. Further downstream, the unsteady heat release rate simply lagged that at the flameholder with a time delay which was also given by the model. When this flame model was combined with a simple linear theory based on a quasi-1D flow analysis, Bloxsidge et al. (1988) were able to predict the buzz frequency and the mode shape of pressure perturbations with reasonable accuracy, but were unable to predict the transition between the two types of instability described above.

Whilst models such as that described by Bloxsidge et al. (1988) are very useful for preliminary analysis of reheat buzz, they will be very difficult to extend to more complicated problems (e.g. involving liquid fuels) and will probably not be able to cope with circumstances where both acoustic response and multi-dimensional fluid mechanical phenomena (e.g. vortex shedding dynamics) combine to control the combustion instabilities. Hence general models for combustion induced oscillations, based on CFD techniques, are required, but are much rarer in the reported literature. One of the few examples is the work of Benelli et al. (1992); these authors used a commercial CFD code (FLUENT) to combine a turbulent combustion model (due to Magnussen and Hjertager (1976)) with a simple model of the unstable feedback loop provided by the oscillating flapper valves in a pulsating combustor. Self-sustaining oscillations were observed when the parameters of the mechanical valve behaviour (e.g. opening delay, pressure loss etc.) were adjusted.

The current paper describes on-going work to develop a CFD model for the buzz-type self-sustained combustion oscillations as reported by LBM. Although future work will extend the analysis to multi-dimensions and explore the sensitivity of results to various forms of turbulence and combustion model, this paper is aimed at confirming that similar predictions as reported by Bloxsidge et al. (1988) can be reproduced within the framework of a general pressure-correction CFD formulation. To this end, the empirical heat-release data from LBM are used to drive a 1D calculation to examine the resulting predictions in view of amplitudes, mode shapes, etc. The present work should be seen therefore as the first step in the development of a general CFD model for reheat-buzz.

MATHEMATICAL MODELLING

Flow Configuration

Figure 1 depicts the geometry for which predictions have been carried out. In essence this represents the experimental configuration used in LBM. Premixed fuel (ethylene C_2H_4) and air at a controlled equivalence ratio are fed through a convergent-divergent nozzle with the throat at x=0 into a cylindrical working section of 70 mm in diameter. The upstream pressure is controlled so that the flow of premixed gas is choked at the throat under the desired running conditions to prevent acoustic disturbances from affecting the mass flow rate condition at the supply. The flame is stabilised in the wake of a conical gutter mounted at a position within the test duct which could be varied to change the upstream (non-reacting) and downstream (reacting) gas column lengths. In order to simplify the application of supply boundary conditions a segment of

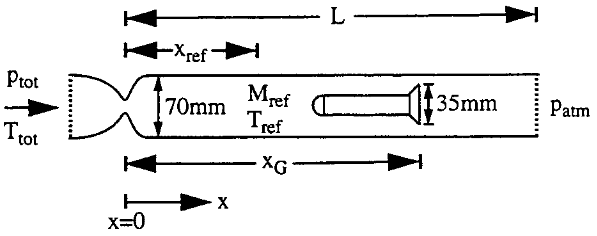

FIGURE 1. SCHEMATIC OF THE BUZZ RIG OF LBM

upstream duct with increasing cross-sectional area has been included. This allows the supply condition to be fixed as given total pressure and temperature to ensure choked throat conditions. Five sets of experimental conditions have been selected from Bloxsidge et al. (1988) for various geometrical conditions and mean approach flow Mach numbers (M_{ref}), and these are summarised in Table 1. Calculations reported below have been based on these five flow configurations.

Table 1: SUMMARY OF FLOW CONFIGURATIONS

configuration No.	1	2A	2B	3	4
duct length L (m)	1.92	1.48		2.18	1.92
gutter lip position x_G (m)	1.18	0.74		1.19	1.18
reference position x_{ref} (m)	0.75	0.49		0.76	0.75
mean Mach number M_{ref} at x_{ref}	0.08	0.08		0.08	0.15
mean temperature T_{ref} at x_{ref}	288K				
equivalence ratio	0.70	0.65	0.66	0.65	0.71
buzz frequency (Hz)	77	81	103	77	109

Governing Equations

The governing equations which have been solved are the non-linear conservation equations of mass, momentum and total enthalpy in quasi-1D form (i.e. averaged over the available duct cross-sectional flow area A whose variation with distance along the duct A(x) is known from the geometry given in Fig. 1):

$$\frac{\partial}{\partial t}(\rho A) + \frac{\partial}{\partial x}(\rho u A) = 0 \qquad (1)$$

$$\frac{\partial}{\partial t}(\rho u A) + \frac{\partial}{\partial x}(\rho u A u) = -A\frac{\partial p}{\partial x} \qquad (2)$$

$$\rho A\frac{\partial h_t}{\partial t} + \rho u A\frac{\partial h_t}{\partial x} = A\frac{\partial p}{\partial t} + q \qquad (3)$$

All diffusion terms arising from molecular and turbulent fluxes have been ignored in the current analysis. The usual notations have been adopted for time, spatial position, velocity, pressure and density; h_t is the total enthalpy per unit mass defined by:

$$h_t = c_p T + u^2/2 \qquad (4)$$

q is a heat source representing the heat released by the combustion process per unit time and per unit length. The set of governing equations is completed by the equation of state:

$$p=\rho RT \qquad (5)$$

where R is the gas constant (taken as 287 J/(kg K)).

Specification Of Unsteady Heat Release

Eqs. (1)-(5) form a closed set only if the instantaneous heat release rate q in Eq. (3) is known as a function of both x and t. To achieve this, data for the time-mean heat release rate, and the amplitude and phase of the unsteady heat release rate as measured by Langhorne (1988) are approximated by a piecewise linear fit. The time dependence of q is assumed to be sinusoidal at a frequency taken from the measured buzz frequency. The reason for the sinusoidal dependency of q on t is that the measured spectra of heat release and pressure were both peaked at the buzz frequency with its harmonics having much smaller magnitudes. In addition, all measured data were for quantities at the buzz frequency. Furthermore, one of the main objectives of this study is to see whether or not the current CFD model can produce the correct unsteady pressure field in response to a given unsteady heat release field.

Figure 2 shows examples of empirically deduced fits for two conditions listed in Table 1. Two fits, one shown as a solid line and one as a dotted line, have been displayed for the phase of unsteady heat release of Configuration 2A. The solid line fit corresponds to the "weak buzz" description by Bloxsidge et al. (1988), while the dotted line fit is just an alternative but more accurate approximation of the measured data point. Note that the experimental data for the amplitude and phase of the unsteady part of heat release are normalised with the measured amplitude of the unsteady pressure signal at the reference location x_{ref}. This is not reported by Bloxsidge et al. (1988), so various values have been tried in the calculations. It was found that predictions were reasonably insensitive to the value chosen as long as this was small enough that the resulting pressure perturbations were within the linear limit (i.e. no harmonics generated in the pressure spectrum). For all calculations reported below a value of 1000 Pascal has been used for p'_{ref}, this gave rise to predicted pressure perturbations at the reference location in the range of 1300 - 2100 Pascal except for Configuration 2A which gave the much smaller value of around 160 Pascal.

Numerical Methods

The above system of equations has been solved using a co-located, finite-volume-based, pressure-correction formulation. Time discretisation has followed a fully implicit approach with Crank-Nicolson averaging for the spatial terms. To ensure adequate resolution of gradients with minimum numerical smearing, the convection terms were discretised using a variant of the MUSCL algorithm as suggested by Anderson et al. (1986). The details of the current scheme will be given shortly. The compressi-

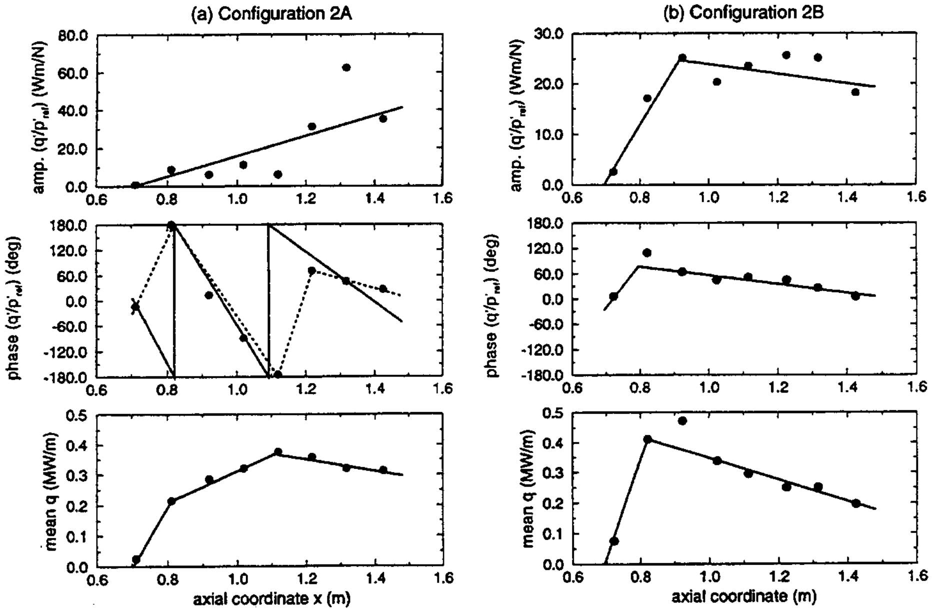

FIGURE 2. SPATIAL VARIATION OF MEAN HEAT RELEASE, PHASE AND AMPLITUDE OF UNSTEADY HEAT RELEASE. ●, EXPERIMENTAL POINTS OF LBM; ——— AND ··············· , LINE FITS.

ble pressure-correction formulation of McGuirk and Page (1990) was adopted to retain good shock-capturing properties of the solver. This included the use of the retarded pressure scheme recommended by McGuirk and Page (1990) in the small region of supersonic flow just downstream of the nozzle throat. Finally, to prevent checkboard-style pressure-velocity decoupling, standard Rhie and Chow (1983) smoothing was included for the cell face mass-flux terms. As mentioned above, upstream (inflow) boundary conditions corresponded to fixed total pressure and temperature and linear extrapolation of static pressure from within the solution domain. The downstream (outflow) condition selected was fixed static pressure (atmospheric since an open-ended duct was used) and linear extrapolation conditions on the momentum component (ρu) and the total enthalpy (h_t). These boundary conditions correspond to the actual experimental conditions of LBM and are clearly NOT non-reflecting. Further, they are consistent with the physics in that the flow is subsonic at both the inflow and the outflow boundaries. Non-uniform grids were used to allow good resolution in steep gradient regions; typically 160 grid nodes were used with 5 nodes upstream of the throat 110 nodes in the non-reacting duct part and 45 nodes downstream of the flame stabiliser. The time step selected was about 5.6 x 10^{-6} s corresponding typically to a cell Courant number of 1. Calculations have shown that use of a finer grid and/or a smaller time step produces negligible difference in the results.

A very satisfactory discretization scheme for the convection terms has been found to be the following. Let the centre of the i-th finite volume cell be at x_i, and the interface between cells i and i+1 be at $x_{i+1/2}$. Then the value of any convected variable, f, at the interface at $x_{i+1/2}$ is computed according to

$$f_{i+\frac{1}{2}} = f_i + \Delta^+ \cdot \left(x_{i+\frac{1}{2}} - x_i\right), \qquad u_{i+\frac{1}{2}} \geq 0 \tag{6}$$

$$f_{i+\frac{1}{2}} = f_{i+1} + \Delta^- \cdot \left(x_{i+\frac{1}{2}} - x_{i+1}\right), \qquad u_{i+\frac{1}{2}} < 0 \tag{7}$$

$$\Delta^+ = minmod\left(\Delta_{i+\frac{1}{2}}, \Delta_{i-\frac{1}{2}}\right) \tag{8}$$

$$\Delta^- = minmod\left(\Delta_{i+\frac{1}{2}}, \Delta_{i+\frac{3}{2}}\right) \tag{9}$$

$$\Delta_{i+\frac{1}{2}} = \frac{f_{i+1} - f_i}{x_{i+1} - x_i} \tag{10}$$

$$minmod(a, b) = s \cdot max(0, min(|a|, s \cdot b)) \tag{11}$$

$$s = \mathrm{sgn}(a) \tag{12}$$

RESULTS

Figure 3 presents example time histories of pressure and heat release rate at selected points upstream and downstream of the flameholder for Configuration 1. The pure sinusoidal forcing frequency of the unsteady heat release produces strong oscillations in

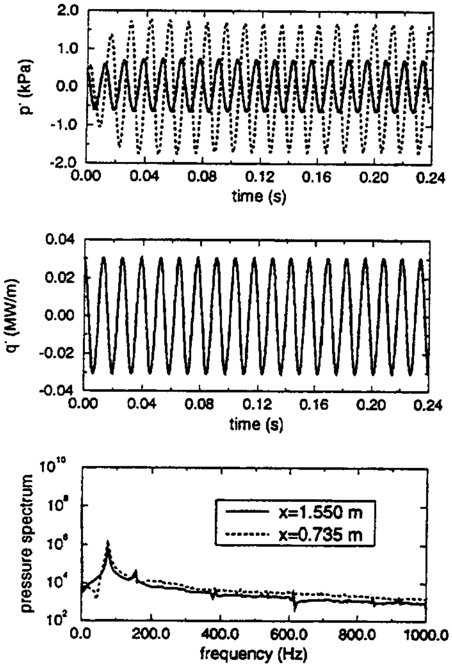

FIGURE 3. TIME HISTORY OF UNSTEADY PRESSURE AND HEAT RELEASE RATE AND CORRESPONDING PRESSURE SPECTRUM.

the pressure field. The amplitude of the pressure oscillation is about three times larger in the upstream position due to the reinforcing nature of the pressure perturbations generated by the unsteady heat release downstream of the gutter. The pressure spectrum shown in Figure 3 indicates that the pressure oscillations are not pure sinusoidal, but the energy is concentrated close to the forcing frequency.

Figures 4 and 5 display pressure and heat release profiles along the duct at twelve instants covering the full cycle of oscillations, again for Configuration 1. Examination of the unsteady heat release contribution (Figure 5)shows that this is only significant for the furthest downstream part of the duct, but this excites pressure waves which propagate throughout the system and alter the pressure field substantially even close to the upstream throat. Over the first quarter of the cycle, even though the heat release rate is decreasing in the downstream portion of the duct, the pressure downstream of the gutter is essentially constant there, but is falling rapidly in the unburnt gas. For the second quarter the heat release rate is rising, as is the pressure in the downstream duct, corresponding to the part of the cycle when energy is input into the oscillations. The pressure is still falling upstream of the gutter, but this trend is reversed over the second half of the cycle where the pressure rises constantly in the upstream unburnt gas. Energy input into the oscillation occurs in the burnt gas also in the third quarter, but seems to be much weaker than in the second quarter.

These unsteady pressure profiles have been processed in the following way to obtain the mode shape and phase of the predicted

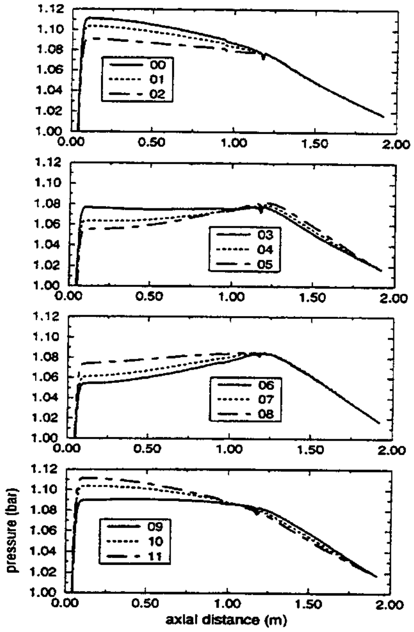

FIGURE 4. INSTANTANEOUS PRESSURE PROFILES AT TWELVE EQUALLY-SPACED TIME INSTANTS COVERING A FULL CYCLE (CONFIGURATION 1).

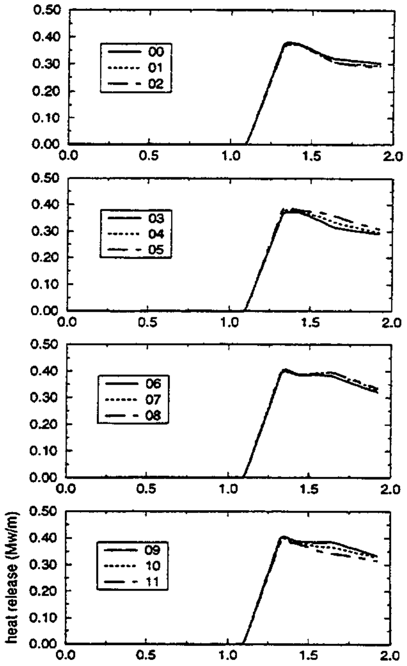

FIGURE 5. INSTANTANEOUS PROFILES OF HEAT RELEASE RATE (SAME CONDITIONS AS FIGURE 4).

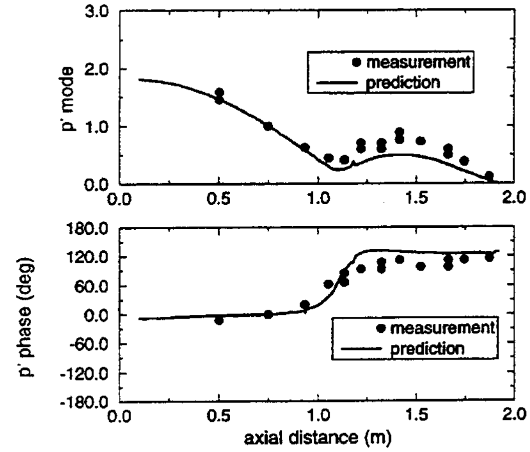

FIGURE 6. PREDICTED PRESSURE MODE SHAPE AND PHASE DISTRIBUTION COMPARED WITH MEASUREMENTS OF LBM (CONFIGURATION 1).

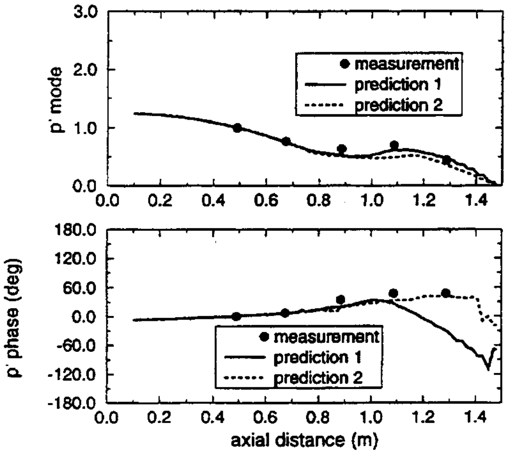

FIGURE 7. PREDICTED PRESSURE MODE SHAPE AND PHASE DISTRIBUTION COMPARED WITH MEASUREMENTS OF LBM (CONFIGURATION 2A).

pressure oscillations. It can be seen from the time histories illustrated in Figure 3 that the pressure perturbations eventually become constant-amplitude oscillations after sufficient time has elapsed. Further, Figure 3 also shows that the oscillation can be treated as a pure sine wave. Pressure mode shapes and phases are calculated after the oscillation has reached the constant-amplitude state. Thus, the pressure mode amplitude at any spatial location is obtained as the difference between the local pressure maximum and the time-averaged value. The phase angle is obtained by considering the pressure perturbations at two consecutive time steps i.e. $p'(x,t)$ and $p'(x,t+\Delta t)$. Defining the acute angle $\alpha = \arcsin[|p'(x,t)|/p'_{max}(x)]$, and the signs $S_1 = \mathrm{sgn}[p'(x,t)]$, $S_2 = \mathrm{sgn}[p'(x,t+\Delta t) - p'(x,t)]$. Then the phase angle is determined as in Table 2.

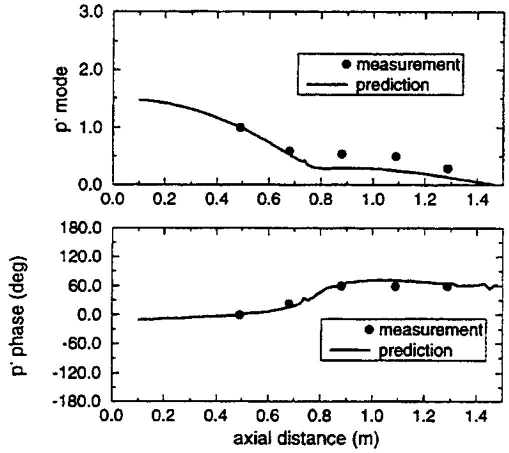

FIGURE 8. PREDICTED PRESSURE MODE SHAPE AND PHASE DISTRIBUTION COMPARED WITH MEASUREMENTS OF LBM (CONFIGURATION 2B).

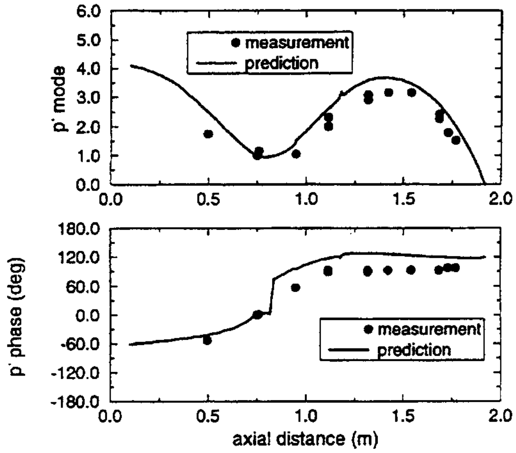

FIGURE 9. PREDICTED PRESSURE MODE SHAPE AND PHASE DISTRIBUTION COMPARED WITH MEASUREMENTS OF LBM (CONFIGURATION 4).

Table 2: DETERMINATION OF PHASE ANGLE

phase ϕ		S_1	
		+	-
S_2	+	α	$2\pi-\alpha$
	-	$\pi-\alpha$	$\pi+\alpha$

Figures 6 to 9 compare the deduced mode shapes and phase distributions with the measurements taken from Langhorne (1988) and Bloxsidge et al. (1988). Good agreement is observed for all configurations, the worst being for Configuration 2A where the

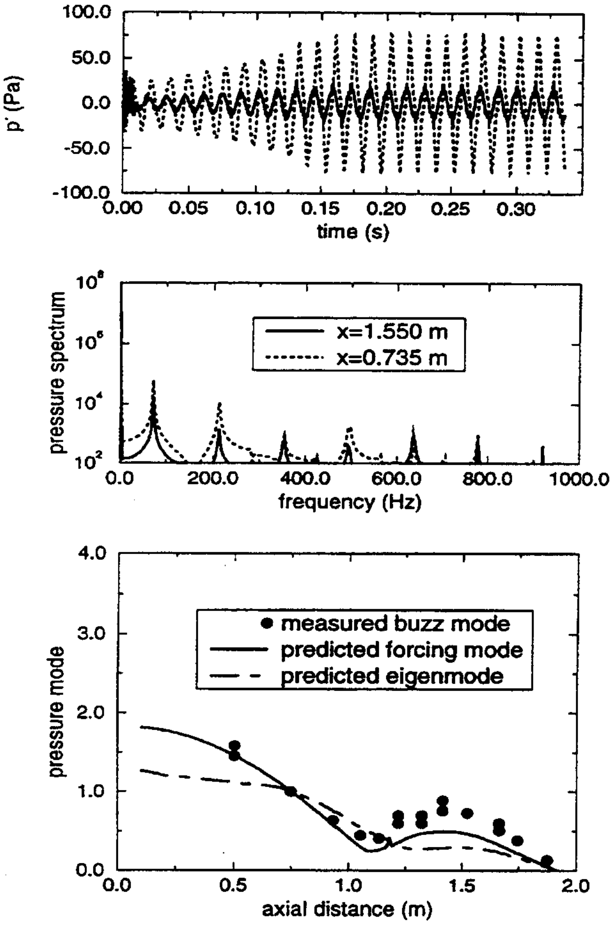

FIGURE 10. TIME HISTORY OF UNSTEADY PRESSURE (TOP) AND CORRESPONDING PRESSURE SPECTRUM (MIDDLE) AND MODE SHAPE (BOTTOM).

predicted phase distribution underestimates the measurements increasingly with downstream distance. This configuration differs from the others in that it was termed "weak buzz" by Bloxsidge et al. (1988); the heat release rate perturbation was assumed to convect downstream from the gutter lip at a constant velocity (leading to a linear decrease in the phase of unsteady heat release rate with downstream distance).This is the basis of the straight line fit to the data shown in Figure 2.The furthest downstream data points for the phase of the heat release do not however agree with a linear phase distribution. In fact the measured phase shows a very slow spatial variation, almost a constant phase, which is more consistent with the "established buzz" model of Bloxsidge et al. (1988). If an almost constant phase is used for the downstream portion (dotted line in Figure 2), the predicted phase distribution for the pressure now agrees well with the measurements (dotted line in Figure 7). This implies that the behaviour in Configuration 2A corresponds to weak buzz in the first half of the duct and established buzz in the second half. The effect of changing the phase distribution on the predicted mode shape is negligible.

The calculations shown in Figures 6-9 indicate that the pressure-correction algorithm is predicting the correct shape and amplitude of pressure oscillations when driven by the empirical heat release data. It is obvious that the CFD model is not predicting the buzz frequency, since this is input as a parameter of the forcing function (heat release). Calculations have shown however that the current CFD model can predict the buzz frequency and also, for the experimental configuration of LBM, that this frequency is essentially the natural acoustic frequency of the flameholder/duct geometry. This may be demonstrated by carrying out calculations with only the steady component of the heat release (i.e. no unsteady forcing present). If this calculation is perturbed (e.g. by the way the calculation is "switched on") then in fact no steady state is predicted because the noise that is generated by the initial perturbation is capable of achieving a self-sustaining state, at least for that frequency content of the noise which corresponds to the natural duct acoustic resonance. Figure 10 shows time histories of the pressure field for one such calculation (Configuration 1), the pressure spectrum and the mode shape (eigenmode) of this naturally self-sustaining oscillation. Although the amplitude is much smaller (by a factor of 30) than that observed when the oscillation is energised by the unsteady heat release, there is still a clearly discernible pressure oscillation at essentially the natural resonant frequency of the system (although the odd harmonics are also present in the pressure spectrum). This frequency may now be said to be a pure prediction of the CFD model. Table 3 shows the eigenfrequencies for all five configurations calculated in this way, compared to the measured buzz frequency of LBM. The trends and agreement are rather encouraging, confirming that the buzz phenomenon in the present experimental conditions is an acoustically determined phenomenon and that the CFD model described is capable of predicting this, as long as the mean heat release is well predicted. Even the difference between Configurations 2A and 2B is reproduced in the predicted eigenfrequencies.

Table 3: EIGENFREQUENCY V. BUZZ FREQUENCY

configuration No.	1	2A	2B	3	4
CFD predicted eigenfrequency (Hz)	71	85	93	67	88
measured buzz frequency (Hz)	77	81	103	77	109

CONCLUSIONS

A CFD study of reheat buzz in a typical laboratory model (as investigated by LBM) has been computed. At this stage the emphasis was on carrying out quasi-1D calculations to confirm that a pressure-correction algorithm (converted to variable density compressible flows) was capable of accurate resolution of the acoustic phenomena which are known to be important in reheat buzz. Using the empirically deduced mean and unsteady heat release data taken from LBM, excellent agreement was observed in terms of pressure time-histories, mode shapes, amplitudes and phase distributions for a range of experimental conditions selected from LBM. It was also demonstrated that the buzz frequencies observed in the experiments were entirely determined by the natural acoustic resonance frequencies of the variable density gas column existing in the duct and defined by the mean heat release data. These calculations are encouraging in that they confirm that a combustion model which is capable of predicting the mean heat release reasonably well will also predict the buzz phenomenon. This is the future direction of the current work, to incorporate a combustion model to replace the empirical heat release data. This will of course have to be done in a multi-dimensional calculation, abandoning the quasi-1D approach used here.

ACKNOWLEDGEMENTS

This work has been carried out within the University Technology Centre in Combustor Aerodynamics at Loughborough University of Technology. The authors would like to acknowledge funding support from the Science and Engineering Research Council (SERC) UK and Rolls-Royce plc. They would also like to ackowledge useful discussions with colleagues at Loughborough, Rolls-Royce plc and DRA (Pyestock).

REFERENCES

AGARD Conference Proceedings No. 450: "Combustion Instabilities in Liquid Fuelled Propulsion Systems," Bath, UK, 1988.

Anderson, W. K., Thomas, J. L., and Van Leer, B., 1986, "Comparison Of Finite Volume Flux Vector Splittings For The Euler Equations," AIAA Journal, vol. 24, pp. 1453-1460.

Benelli, G., De Michele, G., Cossalter, V., Da Lio, H., and Rossi, G., 1992, "Simulation of Large Non-linear Thermo-Acoustic Vibrations in a Pulsating Combustor," 24th Symposium (International) on Combustion, The Combustion Institute, pp. 1307-1313.

Bloxsidge, G. J., Dowling, A. P., and Langhorne, P. J., 1988, "Reheat Buzz: An Acoustically Coupled Combustion Instability. Part 2. Theory," Journal of Fluid Mechanics, vol. 193, pp. 445-473.

Katsuki, M., and Whitelaw, J. H., 1986, "The Influence Of Duct Geometry On Unsteady Premixed Flames," Combustion And Flame, vol. 63, pp. 87-94.

Langhorne, P. J., 1988, "Reheat Buzz: An Acoustically Coupled Combustion Instability. Part 1. Experiment," Journal of Fluid Mechanics, vol. 193, pp. 417-443.

McGuirk, J. J., 1990, "Subsonic Combustor Flow Modelling - State of The Art of CFD Techniques For Reacting And Combusting Flow," In: VKI Lecture Series 1990-02, Gas Turbine Combustion.

McGuirk, J. J., and Page, G. J., 1990, "Shock Capturing Using A Pressure-Correction Method," AIAA Journal, vol. 28, pp. 1751-1757

MacQuisten, M. A., and Dowling, A. P., 1993, "Low-frequency Combustion Oscillations In A Model Afterburner," Combustion and Flame, vol. 94, pp. 253-264.

Magnussen, B. F., and Hjertager, B. H., 1976, "On Mathematical Modelling Of Turbulent Combustion With Special Emphasis On Soot Formation And Combustion," 16th Symposium (International) on Combustion, The Combustion Institute. pp. 719-729.

Rayleigh, J. W. S., 1896, "The Theory of Sound," Macmillan.

Rhie, C. M., and Chow, W. L., 1983, "Numerical Study Of The Turbulent Flow Past An Airfoil With Trailing Edge Separation," AIAA Journal, vol. 21, pp. 1525-1532.

Sivasegaram, S., and Whitelaw, J. H., 1987, "Oscillations in Confined Disc-Stabilised Flames," Combustion and Flame, vol. 68, pp. 121-129.

Yu, K. H., Trouve, A., and Daily, J. W., 1991, "Low-frequency Pressure Oscillations in a Model Ramjet Combustor," Journal of Fluid Mechanics, vol. 232, pp. 47-72